Pis'ma v ZhETF, vol. 102, iss. 9, pp. 701 – 704

Phase stability of α-, γ-, and ε-Ce: DFT+DMFT study

A. O. Shorikov[+*1)], *S. V. Streltsov*[+*], *M. A. Korotin*[+], *V. I. Anisimov*[+*]

[+]*Miheev Institute of Metal Physics UB of the RAS, 620137 Yekaterinburg, Russia*

[*]*Yeltsin Ural Federal University, 620002 Yekaterinburg, Russia*

Submitted 21 September 2015

We present the total energy calculation of α-, γ-, ε-Ce phases in the frame of GGA, GGA+U, and DFT+DMFT methods. It was shown that taken into account of Coulomb correlations in the frame of dynamical mean-field theory allows to reproduce the phase diagram of Ce in correct way. Equilibrium volume calculated within the DFT+DMFT method for face-centered cubic (fcc) structure agrees with experimental Ce-γ cell volume. With temperature decrease energy minimum shifts toward α cell volume. Moreover, the DFT+DMFT total energy for body-centered tetragonal (bct) structure becomes smaller than for fcc one with increase of pressure in agreement with experimental phase diagram. Importance of accounting of Coulomb correlation in the frame of DMFT is discussed.

DOI: 10.7868/S0370274X15210092

Rich phase diagram of cerium draws researchers attention over past 50 years, and the isostructural $\alpha-\gamma$ transition in Ce is one of the classical problems in the modern solid state physics. In the low temperature α-phase (up to $T \sim 100$ K at normal conditions, or for $T \lesssim 300$ K for $P = 1$ GPa) Ce behaves like a Pauli paramagnet, while in the high temperature γ-phase magnetic susceptibility approximately follows the Curie–Weiss law [1]. The transition is accompanied by a drastic volume collapse (9–15 %) [1] and dramatic changes of the electronic spectra [2]. With constant temperature and increasing pressure Ce undergoes the transition from face-centered cubic (fcc) α or γ to orthorhombic $\alpha\prime$ and then monoclinic α'' and body-centered tetragonal (bct) ε-phase (see Fig. 1). In the present work phase stability of Ce in the α-, γ-, and ε-phases was investigated.

Phase transition, spectral and optical properties of Ce metal were investigated previously intensively by both DFT and DFT+DMFT methods. Crystallographic phase transition from fcc to bct was found at 10 GPa in frames of GGA approximation [4] but equlibrium volume of fcc-Ce was underestimated [5]. Critical pressure of $\alpha-\gamma$ transition found in frames of SIC-LSD [6] -2.3 kbar is in satisfactory agreement with experimental value -7 kbar. Note, that DFT also fails to reproduce Ce spectral properties such as quasiparticle peak near Fermi level and Hubbard bands.

The DFT+DMFT with different solvers was applied to investigate Ce problem. Correct tree-peak shape

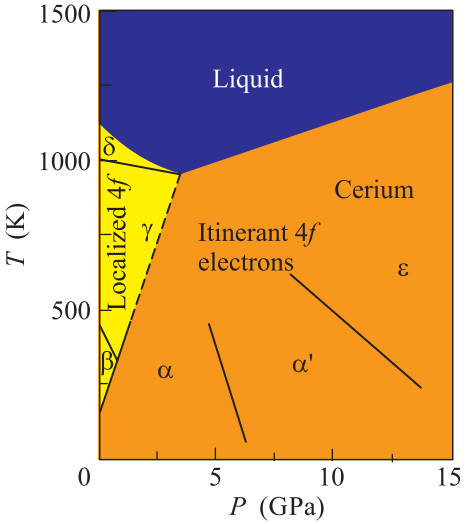

Fig. 1. (Color online) Experimental phase diagram of Ce (taken from Ref. [3])

of of α- and γ-Ce spectra (lower and upper Hubbard bands and also sharp peak near the Fermi level) was reproduced by perturbation theory within non-crossing approximation (NCA) [7]. Good agreement between theoretical and experimental optical spectra was achieved within one-crossing approximation (OCA) [8]. LDA+DMFT method with HF-QMC (quantum Monte-Carlo method with Hirsch–Fay algorithm) solver was used to understand the mechanism of $\alpha-\gamma$ transition [9]. But the calculation was carried out at relatively high temperatures. Magnetic susceptibility of Ce was calculated using DFT+DMFT method with CT-QMC impurity solver [10]. It was shown that calculated magnetic

[1)]e-mail: shorikov@imp.uran.ru

susceptibility in the frame of GGA+DMFT method for the α- and γ-phases of Ce exhibits a qualitatively similar behavior in both phases and should be described by the same model. The role of $f-f$ hybridization in formation of quasiparticle peak in Ce was investigated in Ref. [11]. The importance of $f-f$ hybridization investigated in the frame of DFT+DMFT method for stabilization of α-phase was also emphasized in Ref. [12].

In order to describe many-particle interactions and α–γ–ε transition in paramagnetic phase we choose state-of-the-art DFT+DMFT method (density functional theory together with dynamical mean-field theory) [13]. This approach was used to investigate a wide class of strongly correlated materials based not only of the $3d-5d$, but also of $4f-5f$ metals and Ce is among them [10, 12, 14]. It was exceptionally useful in the study of the structure phase transitions under pressure [15–18]. The calculation scheme is constructed in the following way. First of all, the non-interacting part of the Hamiltonian, $H_{\rm DFT}$, is produced using one of the DFT codes, then the many-body Hamiltonian is set up, and finally corresponding self-consistent DMFT equations are solved.

Ab initio DFT and DFT+U [19] calculations were performed using the pseudopotential plane-wave method and the generalized gradient approximation – GGA [20] (so that corresponding realization of the DFT+DMFT method is referred to as GGA+DMFT), as implemented in the Quantum ESPRESSO package [21]. The Wannier function (WF) projection procedure as described in Ref. [22] was applied to construct $H_{\rm DFT}$. The WFs are defined by the choice of Bloch functions Hilbert space and by a set of trial localized orbitals that will be projected on these Bloch functions. The basis set includes s-, p-, d-, and f-states of Ce.

The resulting Hamiltonian to be solved by the DMFT is written as:

$$\hat{H} = \hat{H}_{\rm DFT} - \hat{H}_{dc} + \frac{1}{2}\sum_{i,\alpha,\beta,\sigma,\sigma'} U^{\sigma\sigma'}_{\alpha\beta}\,\hat{n}^{f}_{i\alpha\sigma}\hat{n}^{f}_{i\beta\sigma'}, \qquad (1)$$

where $U^{\sigma\sigma'}_{\alpha\beta}$ is the Coulomb interaction matrix, $\hat{n}^{f}_{i\alpha\sigma}$ is the occupation number operator for impurity f-states, α,β are orbital and σ,σ' spin indices on the i-th site. The term $\hat{H}_{dc}$ stands for the $f-f$ interaction already accounted in the DFT, so called double-counting correction. In the present calculation the double-counting was chosen in the following form: $\hat{H}_{dc} = \bar{U}(n_{\rm DMFT} - \frac{1}{2})\hat{I}$. Here, $n_{\rm DMFT}$ is the self-consistent total number of f electrons obtained within the DFT+DMFT, $\bar{U}$ is the average Coulomb parameter for the f shell and $\hat{I}$ is unit operator.

The on-site Coulomb repulsion parameter (U) was estimated to be 6.0 eV using a constrained LDA method [23] on Wannier functions [22]. The intra-atomic Hund's rule coupling was set to $J_H = 0$ eV for the sake of simplicity since Ce has only one electron in the f shell.

The effective impurity problem in the DMFT was solved by the hybridization expansion Continuous-Time Quantum Monte-Carlo method (CT-QMC) [24]. Calculations for all volumes were performed in the paramagnetic state at the inverse temperatures $\beta = 1/T = (10-20)\,{\rm eV}^{-1}$ corresponding to 1160–580 K for α–ε transition and $10–60\,{\rm eV}^{-1}$ (1160–190 K) in α–γ case. Spectral functions on real energies were calculated by Maximum Entropy Method (MEM) [25].

Self-consistent GGA+DMFT calculations were performed for several unit cells with *fcc* and *bct* crystal structures for the number of cell volumes. The method of total energy calculation is described in Ref. [18].

At first we have carried out GGA and GGA+U calculation of total energy vs. volume of *fcc*-Ce (see Fig. 2). It's well known that the local density approximation

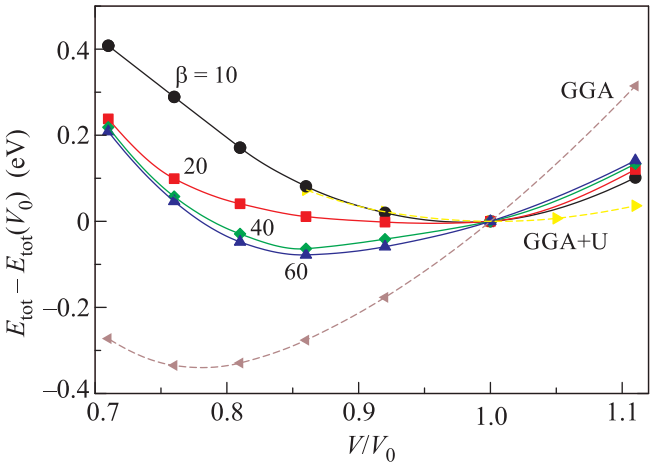

Fig. 2. (Color online) The GGA, GGA+U, and GGA+DMFT total energies of *fcc*-Ce vs. cell volume, where V_0 is experimental γ-Ce volume

(LDA) typically used in the DFT calculations underestimates equilibrium volume, since it tends to have as much homogeneous electron density as possible. In contrast, the GGA is based on the exchange-correlation functional, which takes into account energy dependence of density gradient, but it is still too simplified, does not treat strong Coulomb correlations in an appropriate way. As a result this approximation also strongly underestimates equilibrium volume for γ-phase. Total energy minimum obtained within the GGA corresponds to $0.78V_0$ (experimental value of Ce-γ volume). Note, that it is lower than experimental value of α-Ce volume.

This means that correlation effects should be explicitly taken into account for correct description of Ce in all phases.

One may see that an account of electron correlations already on the GGA+U level markedly improves the results of the calculations. The GGA+U total energy vs. volume curve exhibits the minimum at slightly higher value than experimental γ-phase volume. One of the important disadvantages of the DFT or DFT+U methods is that all calculations are performed for $T = 0\,\mathrm{K}$ and the temperature dependence of all physical properties could be taken into account only via the temperature dependence of the crystal structure. In contrast, temperature explicitly enters to all DMFT equations.

The DFT+DMFT calculations were carried out for four temperatures, corresponding to $\beta = 10\,\mathrm{eV}^{-1}$ (1160 K), $20\,\mathrm{eV}^{-1}$ (580 K), $40\,\mathrm{eV}^{-1}$ (290 K), and $60\,\mathrm{eV}^{-1}$ (190 K). The results of the GGA+DMFT calculations for fcc unit cell are shown in Fig. 2. In the excellent agreement with experiment the minimum of total energy at high temperature ($\beta = 10\,\mathrm{eV}^{-1}$) was obtained at volume corresponding to γ-Ce. Lowering the temperature the equilibrium volume also decreases and gets close to α-Ce volume at $\beta = 40\,\mathrm{eV}^{-1}$ (290 K).

Next we consider the phase transition in Ce upon a very high pressure. In this study we did not consider the transition from fcc-phases (α and γ) to orthorhombic $\alpha\prime$ and monoclinic α'' phases for the sake of simplicity. Moreover, both phases realizing in a narrow range of pressure therefore we focus on the last, bct ε-phase.

The space group of ε-Ce is I4/mmm with unit cell parameters $a = 2.92\,\text{Å}$, $c = 4.84\,\text{Å}$ ($c/a = 1.66$) at 17.5 GPa and $c/a = 1.63$ at 12.1 GPa [26]. Experimental value of α- and ε-Ce volume vs. pressure is shown in Fig. 3 with black circles. In order to investigate phase transition from fcc into bct structures 12 unit cells (6 bct and 6 fcc) were considered. The volumes of the cells correspond to experimental values for α-Ce at 5.6 GPa and ε-Ce at 13 and 17 GPa. For the region between 5.6 and 13 GPa where α' and α'' phases exist unit cell parameters for both fcc and bct crystal structures where obtained using linear interpolation.

The GGA+DMFT total energy for bct- and fcc-Ce vs. temperature and cell volume is shown in Fig. 3. The calculations for all unit cells (pressure values) were performed for two temperatures $\beta = 10^{-1}\,\mathrm{eV}$ (1160 K) and $20^{-1}\,\mathrm{eV}$ (580 K). In accord with the experimental data [3] the bct-structure has the lowest total energy in the DFT+DMFT calculation for the cell volume corresponding to ε-phase. With increase of cell volume (decreasing of pressure) the total energy of fcc-structure becomes lower. This agrees with experimental phase diagram. The same effect of the fcc-structure stabilization occurs with decrease of temperature (critical volume is $22.205\,\text{Å}^3$ at $\beta = 10^{-1}\,\mathrm{eV}$ (1100 K) and $21.465\,\text{Å}^3$ at $\beta = 20^{-1}\,\mathrm{eV}$ (560 K)).

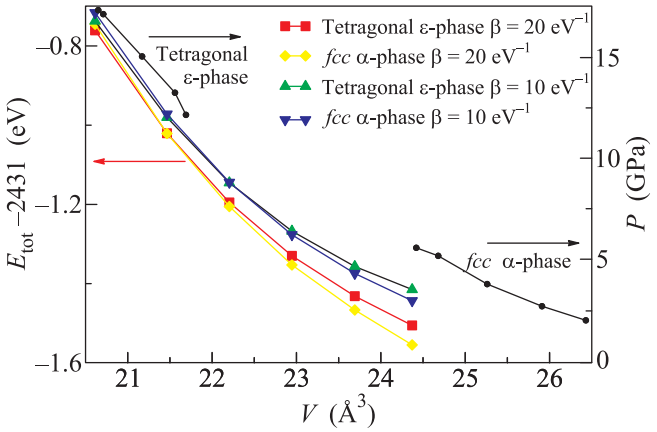

Fig. 3. (Color online) The GGA+DMFT total energy of bct- and fcc-Ce vs. cell volume. Black circles corresponds to experimental data of unit cell volume vs. pressure taken from Ref. [26]

The DFT+DMFT method allows to describe phase diagram of Ce in the best way in comparison with GGA and GGA + U approaches. Calculated temperature dependence of the total energy for fcc-structure demonstrates that equilibrium volume value coincides with experimental Ce-γ cell volume. With the same parameters energy minimum shifts toward α cell volume with decrease of temperature. Comparison of the GGA+DMFT total energy calculated for bct- and fcc-structures at number of pressure values shows that in agreement with experimental phase diagram bct ε-phase becomes stable with pressure decrease.

The GGA+DMFT calculations were performed using Uran supercomputer of IMM UB RAS. Some libraries of the ALPS Project were used in the calculations [27]. The research was carried out within the state assignment of FASO of Russia (theme Electron # 01201463326), supported in part by Russian Foundation for Basic Research (Project # 13-02-00050 and 13-02-00374-a), and Ural branch of Russian Academy of Science via program 15-8-2-4. The work was partially supported by Act 211 Government of the Russian Federation, contract # 02.A03.21.0006.

1. D. Koskenmaki and K. A. Gschneidner, *Handbook on the Physics and Chemistry of Rare Earths*, Elsevier, Amsterdam (1978), ch. 4.
2. L. Z. Liu, J. W. Allen, O. Gunnarsson, N. E. Christensen, and O. K. Andersen, Phys. Rev. B **45**(16), 8934 (1992).

3. B. Johansson and S. Li, J. All. Comp. **444, 445**, 202 (2007).
4. P. Söderlind, O. Eriksson, B. Johansson, and J. Wills, Phys. Rev. B **52**(18), 13169 (1995).
5. P. Söderlind, O. Eriksson, B. Johansson, and J. Wills, Phys. Rev. B **50**(11), 7291 (1994).
6. M. Lders, A. Ernst, M. Däne, Z. Szotek, A. Svane, D. Ködderitzsch, W. Hergert, B. L. Györffy, and W. M. Temmerman, Phys. Rev. B **71**, 205109 (2005).
7. M. B. Zölfl, I. A. Nekrasov, Th. Pruschke, V. I. Anisimov, and J. Keller, Phys. Rev. Lett. **87**, 276403 (2001).
8. K. Haule, V. Oudovenko, S. Y. Savrasov, and G. Kotliar, Phys. Rev. Lett. **94**, 036401 (2005).
9. K. Held, A. K. McMahan, and R. T. Scalettar, Phys. Rev. Lett. **87**, 276404 (2001).
10. S. Streltsov, E. Gull, A. Shorikov, M. Troyer, and V. Anisimov, Phys. Rev. B **85**, 195109 (2012).
11. S. V. Streltsov, A. O. Shorikov, and V. I. Anisimov, JETP Lett. **92**, 543 (2010).
12. B. Amadon and A. Greasier, Phys. Rev. B **91**, 161103 (2015).
13. V. I. Anisimov, A. I. Poteryaev, M. A. Korotin, A. O. Anokhin, and G. Kotliar, J. Phys.: Cond. Mat. **9**(35), 7359 (1997).
14. B. Amadon, S. Biermann, A. Georges, and F. Aryasetiawan, Phys. Rev. Lett. **96**, 066402 (2006).
15. J. Kunes, A. V. Lukoyanov, V. I. Anisimov, R. T. Scalettar, and W. E. Pickett, Nat. Mat. **7**, 198 (2008).
16. J. Kunes, Dm. M. Korotin, M. A. Korotin, V. I. Anisimov, and P. Werner, Phys. Rev. Lett. **102**, 146402 (2009).
17. A. O. Shorikov, Z. V. Pchelkina, V. I. Anisimov, S. L. Skornyakov, and M. A. Korotin, Phys. Rev. B **82**, 195101 (2010).
18. I. Leonov, A. I. Poteryaev, V. I. Anisimov, and D. Vollhardt, Phys. Rev. Lett. **106**, 106405 (2011).
19. V. I. Anisimov, F. Aryasetiawan, and A. I. Lichtenstein, J. Phys.: Cond. Mat. **9**, 767 (1997).
20. J. P. Perdew, in *Electronic Structure of Solids*, ed. by P. Ziesche and H. Eschrig, Akademie Verlag, Berlin (1991); J. P. Perdew, K. Burke, and Y. Wang, Phys. Rev. B **54**, 16533 (1996); J. P. Perdew, K. Burke, and M. Ernzerhof, Phys. Rev. Lett. **77**, 3865 (1996).
21. S. Baroni, S. d. Gironcoli, A. D. Corso, and P. Giannozzi, http://www.pwscf.org.
22. D. Korotin, A. V. Kozhevnikov, S. L. Skornyakov, I. Leonov, N. Binggeli, V. I. Anisimov, and G. Trimarchi, Euro. Phys. J. B **65**(1), 91 (2008).
23. P. H. Dederichs, S. Blügel, R. Zeller, and H. Akai, Phys. Rev. Lett. **53**, 2512 (1984); O. Gunnarsson, O. K. Andersen, O. Jepsen and J. Zaanen, Phys. Rev. B **39**, 1708 (1989); V. I. Anisimov and O. Gunnarsson, Phys. Rev. B **43**, 7570 (1991).
24. P. Werner, A. Comanac, L. de Medici, M. Troyer, and A. Millis, Phys. Rev. Lett. **97**(7), 076405 (2006).
25. M. Jarrell and J. E. Gubernatis, Phys. Rev. **269**, 133 (1996).
26. S. Endo, H. Sasaki, and T. Mitsui, J. Phys. Soc. Jpn. **42**(3), 882 (1977).
27. http://alps.comp-phys.org/. A. Albuquerque, F. Alet, P. Corboz, P. Dayal, A. Feiguin, S. Fuchs, L. Gamper, E. Gull, S. Gürtler, A. Honecker, R. Igarashi, M. Körner, A. Kozhevnikoi, A. Läuchli, S. R. Manmana, M. Matsumoto, I. P. McCulloch, F. Michel, R. M. Noack, G. Pawłowski, L. Pollet, T. Pruschke, U. Schollwöck, S. Todo, S. Trebst, M. Troyer, P. Werner, and S. Wessel, J. Mag. Mag. Mat. **310**, 1187 (2007); B. Bauer, L. D. Carr, H. G. Evertz, A. Feiguin, J. Freire, S. Fuchs, L. Gamper, J. Gukelberger, E. Gull, S. Guertler, A. Hehn, R. Igarashi, S. V. Isakov, D. Koop, P. N. Ma, P. Mates, H. Matsuo, O. Parcollet, G. Pawłowski, J. D. Picon, L. Pollet, E. Santos, V. W. Scarola, U. Schollwöck, C. Silva, B. Surer, S. Todo, S. Trebst, M. Troyer, M. L. Wall, P. Werner, and S. Wessel, J. Stat. Mech. **2011**, P05001 (2011).